

Title	PCB embedded bondwire inductors with discrete thin film magnetic core for power supply in package
Authors	Kulkarni, Santosh;Li, Dai;Jordan, Declan;Wang, Ningning;Ó Mathúna, S. Cian
Publication date	2018-01-29
Original Citation	Kulkarni, S., Li, D., Jordan, D., Wang, N. and O'Mathuna, C. (2018) 'PCB Embedded bondwire inductors with discrete thin film magnetic core for Power Supply in package', IEEE Journal of Emerging and Selected Topics in Power Electronics, 6(2), pp. 614-620. doi: 10.1109/JESTPE.2018.2799238
Type of publication	Article (peer-reviewed)
Link to publisher's version	10.1109/JESTPE.2018.2799238
Rights	© 2018 IEEE. Personal use of this material is permitted. Permission from IEEE must be obtained for all other uses, in any current or future media, including reprinting/republishing this material for advertising or promotional purposes, creating new collective works, for resale or redistribution to servers or lists, or reuse of any copyrighted component of this work in other works.
Download date	2023-05-04 20:06:59
Item downloaded from	<a href="http://hdl.handle.net/10468/5553">http://hdl.handle.net/10468/5553</a>



# UCC

**University College Cork, Ireland**  
Coláiste na hOllscoile Corcaigh

# PCB Embedded bondwire inductors with discrete thin film magnetic core for Power Supply in package

*Santosh Kulkarni<sup>1</sup>, Member, IEEE, Dai Li<sup>1</sup>, Declan Jordan<sup>1</sup>, Ningning Wang<sup>1,3</sup>, Member, IEEE, Cian O'Mathuna<sup>1,2</sup>, Fellow, IEEE*

<sup>1</sup> Microsystems Centre, Tyndall National Institute, University College Cork, Ireland

<sup>2</sup>Department of Electrical and Electronic Engineering, University College Cork, Ireland

<sup>3</sup>Sengled, Jiaxing, China

Corresponding author

Santosh Kulkarni

Microsystems Centre, Tyndall National Institute, University College Cork, Ireland

**Tel:** (353) 21-2346249

**Email:** Santosh.kulkarni@tyndall.ie

**ABSTRACT**—This paper details the design, assembly, and detailed characterization of Printed Circuit Board (PCB) embedded thin magnetic film inductor for Power Supply in Package applications. Solenoidal inductors were assembled on copper tracks printed on PCB with wire bonds to complete the copper loop. Further, the solenoid inductors have laminated amorphous soft magnetic thin films embedded between the two conductor layers. The devices have chemically thinned Vitrovac films laminated as core material. Three different designs of solenoid inductors with different number of turns, are assembled and characterized. The assembled PCB inductor measured a highest Quality factor of 8.5 for a 3 turn device at 10 MHz.

**Index Terms**— PCB based Magnetic devices, switched-mode power supply, thin film magnetic core, integrated circuits, power inductors, power conversion

## I. INTRODUCTION

Recent trends in the area of low power dc-dc converters have focused on miniaturization and increased power density for these devices. The increase in power densities and reduction in device footprint can be achieved to increased switching frequencies. Increased switching frequencies leads to lower energy storage requirements in the power circuit, resulting in lower inductance for the same ripple current in the circuit. Where the required inductance is sufficiently low, the inductor structures can be integrated on to different substrates including semiconductor based i.e, Silicon and Printed Circuit Board (PCB). The silicon based devices are typically designed for very high frequency operation ( $>20\text{MHz}$ ), requiring more advanced switch technology, whereas the PCB based inductors can be efficiently designed for low-medium frequency range ( $<10\text{ MHz}$ ). However, in order to achieve the device miniaturization, thin magnetic films with high saturation magnetization have to be integrated on the PCB substrate.

Much of the previous work in the area of PCB magnetics have focused on developing different inductor structures including racetrack, spiral, toroidal [1-6]. In recent years, the researchers have investigated implementation of planar inductor structures without magnetic cores [7,8]. The air core inductors while being efficient require large footprint or volume in order to provide necessary inductance or need the converter to operate at very high frequencies to meet the footprint specifications, which would in turn require expensive advanced CMOS switches to achieve efficiencies of  $>90\%$  for overall converter. An alternate approach would be to introduce magnetic

cores in the PCB inductors to improve their inductance density and allow switches to operate at lower frequencies. However, including magnetic cores in PCB process is complex and challenging, few reports use ferrite cores on top and bottom of spiral windings on PCB [5]. Use of ferrite cores with low saturation flux density results in larger volume devices which do not benefit from switching at higher frequencies. Hence, the need is to introduce soft magnetic thin film cores with high saturation flux density to achieve the target of higher inductance density and smaller footprint. Earlier reports in this area were focused on realizing a planar winding construction sandwiched between two magnetic layers [9]. However, the disadvantage of this approach is that it is difficult to introduce uniaxial anisotropy in the core, which is required for high frequency operation.

An alternate approach to realizing inductor structures on package is using wire bonding technology to close the current loops. This technology offers advantage of lower DC resistance and higher Q-factor for devices, apart from being more reliable and easy to implement. Further to improve reliability and performance, the wirebond can be replaced by Cu clips which provide more consistent results in comparison to wire bonds. A number of publications have been reported on bond wire inductors with magnetic epoxy as core material [3, 10, 11, 12]. However, use of magnetic powder based epoxy as core material does not provide the required miniaturization in terms of device size, due to the lower saturation flux density of the epoxy material. In a recent work [5], a toroid inductor using a tape wound  $20\text{ }\mu\text{m}$  thick amorphous soft magnetic thin films (Vitrovac 6155) was used to demonstrate a PFC circuit. However, the  $20\text{ }\mu\text{m}$  thickness of soft magnetic thin films limits the

device to 100's of KHz due to eddy current losses in the core material.

In this paper, we report design, assembly and characterization of three different solenoid devices on PCB. The devices are 3 turn, 4 turn and 5 turn designs with copper tracks printed on PCB substrate with wirebonds completing the conductor loop. A typical example of the PCB based device is shown in Figure 1. The device use a chemically thinned Vitrovac 6155 (5 $\mu$ m thick) laminated stack as core material. The devices show a peak DC quality factor ( $L_{dc}/R_{dc}$ ) of 2.3 nH/m $\Omega$  for 5 turn device and peak AC quality factor of 8.5 @ 10 MHz for 5 turn device. The 3 turn and 4 turn device show good frequency response upto 30 MHz making them ideal candidates for Power Supply in package applications. The designs in this study were considered based on the capability of PCB manufacturing partner and also the packaging capability in our lab.

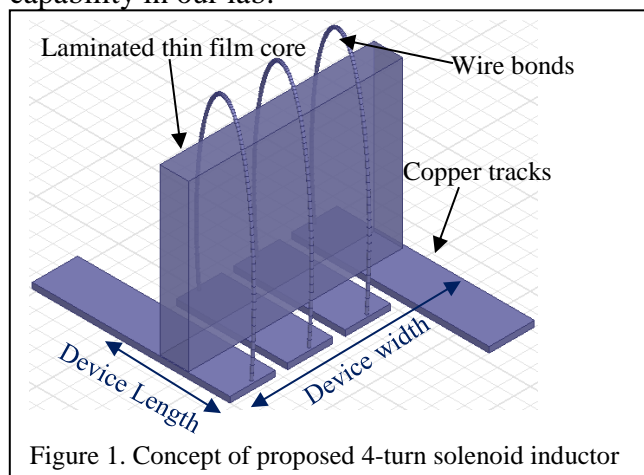


Figure 1. Concept of proposed 4-turn solenoid inductor

The paper will first describe the characterization of thinned Vitrovac 6155 films for power loss density at different frequencies from 100 kHz to 1 MHz in Section II. In Section III, details the design and assembled solenoid inductors using the thinned Vitrovac 6155 films as core material. Section IV explains the characterization of the assembled devices. Conclusions are summarized in Section V.

## II. THINNED VITROVAC 6155 FOR HIGH FREQUENCY POWER APPLICATIONS

In our previous publication [13], we demonstrated an accurate technique for characterizing the large signal power loss performance of soft magnetic thin films. Further, in that report we also showed the lowest power loss density of all soft magnetic thin film materials reported in literature, thinned

Vitrovac 6155. The film thickness was reduced from 21 $\mu$ m to 5 $\mu$ m using chemical etching technique. Figure 2 shows the power loss density of thinned (5 $\mu$ m thick) Vitrovac 6155 at three different frequencies (100 kHz, 500 kHz and 1 MHz) with varying peak ac flux densities in the material. The films are assembled in form of a tape wound toroid with 25 turns of primary and secondary wound around the core material forming a transformer device. The loss in the tape wound core is measured by supplying primary current and measuring secondary voltage. An equivalent air core transformer is also connect in the circuit to compensate of the air coupling in the core material, as explained in our previous publication [13].

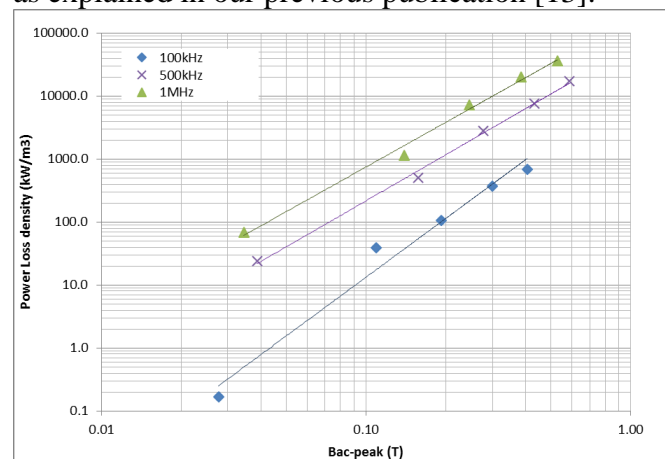


Figure 2. Power loss density of Vitrovac 5 $\mu$ m thick material at different frequencies and applied ac fields. From the plot, the power loss density of the thinned Vitrovac film is 800 kW/m<sup>3</sup> at 0.1 T peak field and 1 MHz frequency, which is one of the lowest power loss density for all soft magnetic core materials. In this work, 6 layers of 5  $\mu$ m thick Vitrovac films were laminated using a 2  $\mu$ m thick cling film tape. Further, if the loss density data is extrapolated to 10 MHz, the loss density varies with frequency to the power of 1.7 ( $P_{lossdensity} \propto Freq^{1.7}$ ), the power loss density at 10 MHz at 0.1 T peak B field is 37 MW/m<sup>3</sup>.

## III. DESIGN OF PCB THIN FILM INDUCTORS

As explained in the earlier sections, three different designs of solenoid inductors with laminated thin film core embedded within the wire bonds were investigated in the work. The three different solenoid designs were for three different winding constructions, with varying number of turns (N). Table 1 summarizes the different winding

constructions investigated, along with their physical dimensions. The copper track thickness was fixed at 35  $\mu\text{m}$ . The bondwire diameter was selected to be 125  $\mu\text{m}$ , as this is the maximum diameter of Aluminum wire from the wedge bonder used in this work.

*Table 1. Summary of the copper and device dimensions investigated in this work*

Structure	Track Width (mm)	Track Spacing (mm)	Device Length (mm)	Device Width (mm)	Footprint (mm <sup>2</sup> )
Design 1- 3 turns	0.55	0.15	1.95	1.29	2.5
Design 2- 4 turns	0.55	0.15	1.95	2.65	5.1
Design 3- 5 turns	0.55	0.15	1.95	3.35	6.5

The design of the thin film inductors was done using Finite Element Analysis (FEM). 3D finite element modelling was performed using Maxwell Ansys v.16 to determine the electrical characteristics of the 3, 4, and 5 turn device with a laminated core. The Eddy Current solver programme of Ansys v16 was employed to simulate the performance of the different designs. The laminated magnetic core consisted of 6 Vitrovac thin films of 5  $\mu\text{m}$  thickness separated by a 2  $\mu\text{m}$  dielectric, with a total core thickness of 40  $\mu\text{m}$ . Table 2 summarize the magnetic properties of the core material as used in the ANSYS simulations. Bondwires were created using a set of parametric equations to form elliptical arcs connecting the copper pads, and enclose the magnetic core. The major and minor arc of the bondwires for the 3, 4, and 5 turn device were 2 mm and 0.85 mm respectively. As explained previously, the diameter of the bondwires were fixed at 125  $\mu\text{m}$ .

*Table 2 Magnetic properties of Vitrovac 6155 thin films used in Ansys 16v simulation*

Device	Core Width (mm)	Core Height (mm)	Core thickness (mm)	Relative permeability, $\mu_r$
Design 1, N=3	2.35	1.75	0.04	2000
Design 2, N=4	2.95	1.75	0.04	2000
Design 3, N=5	3.55	1.75	0.04	2000

The results of the simulation are summarized in Table 3. The Eddy Current solver programme computes the total energy stored in the device including the flux stored in the core material and in the air. The stored energy value is then calculated

by dividing the energy stored with the square of the RMS current used in the simulation. In this case, both air core and magnetic core inductances for the different designs have been simulated. The simulated inductance values are consistent with the analytical models where the inductance varies with square of the number of winding turns. For example, the inductance from 3 turns to 4 turns device should increase by  $35 \times (4)^2 / (3)^2 = 62\text{nH}$  and similarly for 3 turns to 5 turns device is  $35 \times (5)^2 / (3)^2 = 98\text{nH}$ , which are close to the simulated values.

Further, based on the modelled inductances, it was estimated that the current handling capability for the 3-turn device is 1.2 A, 4-turn device is 1 A and 5-turn device is 0.75A.

*Table 3 Simulated inductances of devices*

Device	Simulated air-core Inductance @ 60 Hz (nH)	Simulated magnetic core Inductance @ 60 Hz (nH)
Design 1, N=3	12	35
Design 2, N=4	16	57
Design 3, N=5	20	105

Based on the simulation results, three different devices were assembled on PCB with different number of turns Design 1(N-3), Design 2(N-4) and Design 3(N-5). The assembled devices were characterized for the electrical performance using impedance analyzer for ac performance. The details of the assembly process and device characterization are explained in the next section.

#### IV. ASSEMBLY AND CHARACTERIZATION OF PCB THIN FILM INDUCTORS

As explained in the previous sections, Vitrovac 6155 thin film material was used as a core material. The commercially available Vitrovac 6155 is around 20  $\mu\text{m}$  thick, limiting the operational frequency of the material is less than 200 kHz, due to eddy current losses. In order to reduce the eddy current losses at higher frequencies, an in-house developed wet etching process was used to reduce



the film thicknesses to 5  $\mu\text{m}$ . The details of this process were published in our previous work [13]. In assembling the prototype, 6 layers of 5  $\mu\text{m}$  thick Vitrovac 6155 were packaged together using a 2  $\mu\text{m}$  cling film as the dielectric separating the different layers. This packaged Vitrovac laminate was used as a core material which was placed in between the wirebonds and the PCB tracks.

The PCB track layouts were designed in Cadence Allegro. The three different track layouts are shown in the figure 3.

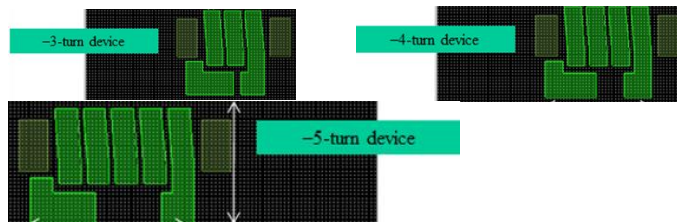


Figure 3. Track layouts for different PCB thin film inductors (a) 3-turn device, (b) 4-turn device, (c) 5-turn device

The surface of based PCB was finished with Electroless Ni/Immersion Au to prevent surface oxidation and make it more suitable for Al wirebonds. The dimensions of the copper tracks were as per the specifications in table 1, with track width and spacing of 550  $\mu\text{m}$  and 150 $\mu\text{m}$ , along with a thickness of the copper tracks were 35  $\mu\text{m}$ . Orthodyne Model 20 wire-bonder, was used to connect the copper tracks using wire bonds. Here, as explained previously, a 125  $\mu\text{m}$  diameter Aluminum wire was used as wire bonds, which was the maximum wirebond diameter available for the wirebonding equipment. In the first instance, these devices were characterized as air core prototypes, using HP 4285 LCR meter for low frequency inductances in order to validate the models. From figure 4 and table 3 a comparison between the modelled air core inductances (60Hz) and measured air core inductance (1 MHz) shows a good match between measured and modelled data for designs 1 and 3.

The difference between the modelled and measured inductance is within the error range associated with imperfect assembly of the devices, in particular for 4 turn device, where the air core inductance is lower than modelled value. This result suggests that 4 turn device has lower wire loop diameter in turn reducing the air core inductance.

The variation of measured inductance against frequency from air core for the three designs is shown in figure 4. The DC resistance for different prototypes were measured to be 30 m $\Omega$  (Design 1-N-3), 40 m $\Omega$  (Design 2-N-4) and 50 m $\Omega$  (Design 3-N-5).

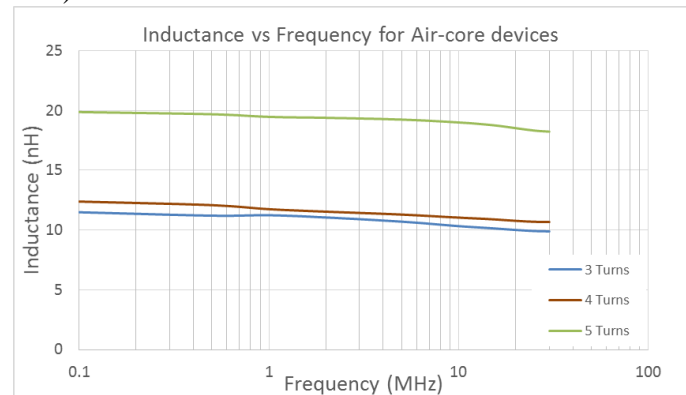


Figure 4. Variation of inductance with frequency for air core devices

Further, a magnetic core made up of laminated Vitrovac 6155 was assembled in between the two windings. Figure below shows the fully assembled prototypes of the three designs.



Figure 5. Fully assembled PCB thin film inductors (a)Design 1(N-3)(b)Design 2(N-4)(c)Design 3(N-5)

As with the air core devices, the magnetic core devices were also characterized for their inductance and resistance upto 30 MHz. Figure 6 shows variation of inductance with frequency of all the different designs.

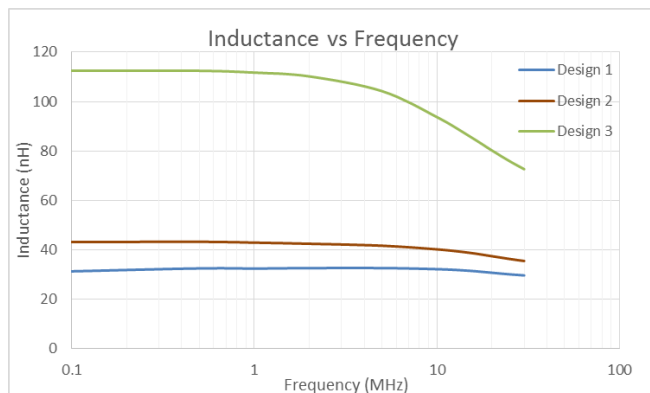


Figure 6. Inductance vs Frequency for Design 1(N-3); Design 2(N-4); Design 3(N-5)

From Figure 6, the inductance values for Design 1 (N-3) and Design 3 (N-5) are close to the simulated values (Design 1- Measured-32.5 nH, Simulated- 35 nH; Design 3- Measured- 114 nH, Simulated- 105 nH). However, Design 2 (N-4) the measured inductance is lower than simulated values (Design 2- Measured- 43 nH, Simulated- 57 nH). The lower value of measured inductance for Design 2 is consistent with measured air core inductance for the same device without a magnetic core. Hence, it is very likely that the assembled prototype for Design 2 (N-4) is different from the modeled structure, likely smaller than simulated structure and this could explain the reason for lower inductance in the measured device as compared to simulated structure.

More interesting to note is the frequency response for three different device prototype, where the inductance drop at higher frequencies (30MHz) is higher for higher coil turns. The inductance drop for Design 1 (N-3) between frequency of 1MHz and 30 MHz is 9%, similarly for Design 2 (N-4) the inductance drop is 20% and finally for Design 3 (N-5) the inductance drop is 55%. In a small signal measurement, as with Impedance Analyzer, the only loss mechanism which is measured is the eddy current losses in core and winding. The eddy current losses in the core material can be calculated using the equation 1,

$$P_e = \frac{\omega^2 \cdot (\mu \cdot H)^2 \cdot t^2}{24 \cdot \rho} \quad (1)$$

The same core structure was employed in all the three device designs, with laminated thinned Vitrovac 6155. From the above equation, the resistivity ( $\rho$ ), core thickness ( $t$ ), applied field ( $H$ )

and frequency ( $\omega$ ), stay the same for all the designs. However, the relative permeability ( $\mu$ ) of the core material does change with the shape and aspect ratio of the core material. The impact of different core shapes on the permeability has been clearly explained in previous reports [17]. The shape anisotropy is a key anisotropy energy which influences the magnetic properties in the soft magnetic thin films in particular the overall material anisotropy field and relative permeability in turn. The shape anisotropy model suggests that the anisotropy energy from shape is highest along the longer edge of the thin film, inducing the magnetic domains to align along the longer edge. This in turn implies that the films with longer edge will have higher anisotropy energy in the longer edge direction and hence align more magnetic domains along the longer edge. This results in lower anisotropy field along the longer edge i.e., less field is required to saturate the material and hence higher relative permeability. The device 3 has the longest edge along the flux path in comparison with device 1 & 2 and hence has highest relative permeability, resulting in faster drop in inductance with frequency in comparison with other two devices. Further, as can be seen from the assembled device in figure 5, there are inconsistencies in terms of bondwire loops from the process, which also impact the device performance. This is due to the limitation of the packaging tool used which is a research scale tool for smaller wires (wire diameter used in this work is the highest possible on the tool).

Using the shape demagnetization model, the change in material permeability with shape can be estimated. Assuming the relative permeability of the material for a 3-turn device is 2000 (2.35 mm\*1.75 mm), then the estimated relative permeability of 4-turn device with core dimensions of 2.95 mm\*1.75mm is 2600. Similarly, the relative permeability of 5-turn device with core dimensions of 3.55 mm\*1.75mm will be 3400. As can be seen from these calculations, increase in aspect ratio of the core results in increased permeability, which in turn results in higher eddy current losses in the core and hence faster drop in inductance with frequency. This explains the reason for different frequency response for different prototypes investigated in this work. This is further confirmed in Figure 7 which shows variation of ac resistance and Q-factor with frequency of all the different designs.

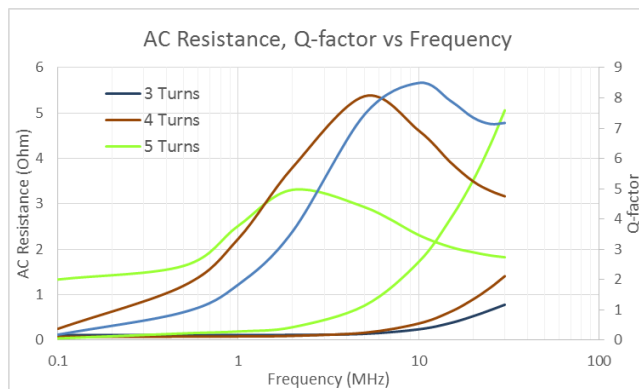


Figure 7. AC Resistance and Q-factor vs frequency for Design 1(N-3); Design 2(N-4); Design 3(N-5)

The AC resistance plot also confirms the impact of shape anisotropy, as the resistance value increases with frequency more dramatically for Design 3 compared to Design 2 & 1. Based on the inductance and resistance measurements, the Q-factor of the devices are plotted in figure 7. The peak Q-factor for the different designs are 8.5 @ 10 MHz (Design 1-N-3), 8 @ 5 MHz (Design 2-N-4) and 5 @ 2 MHz (Design 3-N-5). The Quality factor of the device depends on the losses within the core material and copper windings at higher frequencies. A key mechanism of core losses is the eddy current losses which depends on the permeability and thickness of the core laminations. The lower Q-factor for the 5-turn device can be explained by the higher relative permeability of the core material. The higher relative permeability results in lower skin depth at different frequencies, which in turn increases the eddy current loss in the core material, thereby reducing Q-factor of the device.

In order to reduce the eddy current losses and improve the Quality factor, the thickness of the individual lamination needs to be reduced below the 5 $\mu$ m thick range reported in this work. Further, if the copper track thickness and bond wire thickness can be increased then corresponding ac losses in the winding can also be reduced, hence increasing the device Q-factor.

The key figures of merit for three devices are also summarized in the table 4.

Table 4. Comparison between three different prototypes using both DC and AC Figure of Merit

Device	DC Figure of Merit $L_{dc}/R_{dc}$ (nH/m $\Omega$ )	AC Figure of Merit – Peak Q factor @ Frequency
Design 1 (N-3)	1.1	8.5 @ 10 MHz
Design 2 (N-4)	1.3	8 @ 5 MHz
Design 3 (N-5)	2.4	5 @ 2 MHz

Design 1 (N-3)	1.1	8.5 @ 10 MHz
Design 2 (N-4)	1.3	8 @ 5 MHz
Design 3 (N-5)	2.4	5 @ 2 MHz

The LCR meter measurement is a small signal test which only characterizes the eddy current losses in the device (core & windings). The device in a real application experience significantly higher current amplitudes, where losses such as a hysteresis and anomalous losses in the core material appear. The impact of these losses is to reduce the Quality factor of device from its small signal value. From this work, a key design learning for similar inductor construction, for improved DC performance, the solenoid should have more windings and longer core width, where as for improved ac performance the device needs to have less windings and longer core length. Further, Figure 8 compares the performance of the PCB assembled devices in this work with other reports on PCB based inductor structures reported in literature.

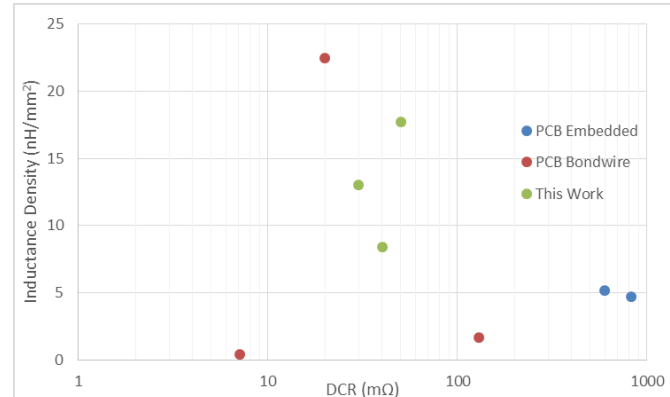


Figure 8. Comparison of different PCB based inductor structures reported in literature

From figure 8, it is clear that the PCB inductors using laminated thin film cores provides reasonably high inductance densities for moderate DCR resistance. This performance can be further improved by using more advanced PCB copper technology and wider diameter bondwires as used in previous work [3, 11, 12].

## V. CONCLUSIONS

This paper presents the design, assembly, and detailed characterization of Printed Circuit Board



(PCB) embedded thin magnetic film inductor for Power Supply in Package applications. Three different solenoidal inductors constructions were modelled using ANSYS Maxwell's 3-D Finite Element Analysis, using copper tracks printed on PCB with bondwires to complete the copper loop. Further, the solenoid inductors have thinned laminated amorphous Vitrovac 6155 thin films embedded between the two conductor layers to improve the inductance density of the devices. The assembled inductors show maximum Ldc/Rdc of

2.4 nH/mΩ) for five turn device and peak Quality factor of 8.5 for a turn turn device at 10 MHz.

#### ACKNOWLEDGMENT

The authors would like to acknowledge funding from Science Foundation Ireland through their Starting Investigator (15/SIRG/3569). Authors also acknowledge the support from Vacuumschmelze in providing thin film material for this work.

#### REFERENCES

- [1] C. O'Mathuna, N. Wang, S. Kulkarni, S. Roy, 'Review of integrated magnetics for Power Supply on Chip (PwrSoC)', *IEEE transactions on Power Electronics*, **27**, 11, 4799-4816 (2012).
- [2] M. Ludwig, M. Duffy, T. O'Donnell, P. McCloskey, C. O'Mathuna, 'PCB Integrated Inductors for Low Power DC-DC converters', *IEEE transactions on Power Electronics*, **18**, 4, 937-945 (2003).
- [3] H. Jia, J. Lu, X. Wang, K. Padmanabhan, J. Shen, 'Integration of a Monolithic Buck Converter Power IC and Bondwire Inductors with ferrite epoxy glob cores', *IEEE transactions on Power Electronics*, **26**, 6, 1627-1630 (2011)
- [4] M. Wang, J. Li, K. Ngo, H. Xie, 'Silicon molding techniques for integrated power MEMS inductors', *Sensors and Actuators A:Physical*, **166**, 157-163 (2011)
- [5] C. Marxgut, J. Muhlethaler, F. Krismer, J. Kolar, 'Multiobjective optimization of ultraflat magnetic components with PCB integrated core', *IEEE transactions on Power Electronics*, **28**, 7, 3591-3602 (2013)
- [6] Z. Zhang, K. D. Ngo, J. Nilles, 'Design of Inductors with significant AC flux', *IEEE transactions on Power Electronics*, **32**, 1, 529-539 (2017)
- [7] E. Burton, G. Schrom, F. Paillet, J. Douglas, W. Lambert, K. Radhakrishnan, M. Hill, 'FIVR- Fully integrated voltage regulators on 4<sup>th</sup> generation INTEL core SOCs', *Applied Power Electronics Conference and Exposition (APEC)*, 432-439 (2014)
- [8] G. Schrom, P. Hazucha, F. Paillet, D. J. Rennie, S. T. Moon, D. S. Gardner, T. Karnik, P. Sun, T. T. Nyuyen, M. J. Hill, K. Radhakrishnan, T. Memioglu, 'A 100 MHz Eight phase buck converter delivering 12A in 25 mm<sup>2</sup> using air-core inductors', *Applied Power Electronics Conference (APEC)*, 727-730 (2007)
- [9] S. O'Reilly, M. Duffy, T. O'Donnell, P. McCloskey, C. O'Mathuna, M. Scott, N. Young, 'New Integrated Planar magnetic cores for inductors and transformers fabricated in MCM-L technology', *International Journal of Microcircuits and Electronic Packaging*, **23**, 1, 62-69 (2000)
- [10] Z. J. Shen, J. Lu, X. Cheng, H. Jia, and X. Gong, "On-chip bondwire inductor with ferrite-epoxy coating: A cost-effective approach to realize power systems on chip," in *Proc. 38th Ann. IEEE Power Electron. Spec. Conf. (PESC)*, Orlando, FL, Jun. 2007, pp. 1599–1604.
- [11] J. Lu, H. Jia, A. Arias, X. Gong, and Z. J. Shen, "On-chip bondwire transformers for power SiP applications," in *Proc. 23rd Ann. IEEE Appl. Power Electron. Conf. Expo. (APEC)*, Austin, TX, Feb. 2008, pp. 199–204.
- [12] J. Lu, H. Jia, A. Arias, X. Gong, and Z. J. Shen, "On-chip bondwire magnetics with ferrite-epoxy glob coating for power systems on chip," *Int. J. Power Manage. Electron.*, p. 9, (2008)
- [13] S. Kulkarni, D. Li, N. Wang, S. Roy, C. Ó Mathúna, G. Young, P. McCloskey, "Low loss Magnetic thin films for off-line power supplies", *IEEE Transactions on Magnetics*, **50**, 1-4, (2014)
- [14] The Radiotron Designer's Handbook, 3rd Edition, 8th Impression, 1942, edited by F. Langford-Smith, Published by The Wireless Press for Amalgamated Wireless Valve, Company pty. Ltd., Sydney, Australia. pp 141-146

- [15] N. Wang, H. Hauser, T. O'Donnell, P. McCloskey, C.O'Mathuna, "Modelling of High Frequency Micro-Transformers", *IEEE Trans. On Magnetics*, **Vol. 40**, No. 4, July 2004, pp 2014-2016.
- [16] Paul J. van Wijnen, "On the Characterization and Optimisation of High-Speed Silicon Bipolar Transistors", Cascade Microtech, INC.
- [17] B. Jamieson, T. O'Donnell, S. Kulkarni, S. Roy, "Shape-independent permeability model for uniaxially-anisotropic ferromagnetic thin films", *Applied Physics Letters*, **96**, 202509 (2010)